Synthetic ground motions at Quebec City from Charlevoix earthquakes using empirical Green's functions

Stephen Crane[1], Claire Perry[1], Dariush Motazedian[2], John Adams[3]

[1] Research Scientist, Canadian Hazards Information Service, Natural Resources Canada - Ottawa, ON, Canada.
[2] Professor and Chair, Department Earth Sciences, Carleton University - Ottawa, ON, Canada.
[3] Seismologist, Canadian Hazards Information Service, Natural Resources Canada - Ottawa, ON, Canada.

ABSTRACT

The Charlevoix Seismic Zone (CSZ), a region spanning approximately 5000 km^2 located about 100 km to the northeast of Quebec City, is the zone of highest seismic hazard in eastern Canada. Five large earthquakes of moment magnitude larger than 6.0 have been documented historically. The latest occurred in 1925 and was recorded on 29 seismograph stations, several in Canada. While none of these historical earthquakes have digital recordings within or near Quebec City, there are many recent seismic records of moderate earthquakes. Seismic provisions for the 2015 National Building Code of Canada (NBCC) as well as historical accounts of damage resulting from the 1925 Charlevoix earthquake suggest that a magnitude 6.0+ earthquake occurring in this seismic zone would cause large and potentially damaging ground motions at Quebec City. In this paper, we use digital recordings of small to moderate earthquakes at local distances sampling the spatial and depth extent of CSZ at station QCQ (Quebec City) to calculate empirical Green's functions. A composite slip model is developed using known CSZ fault geometries to create random slip distributions on a rupture plane. The rupture plane is randomly placed on one of the two-modelled fault planes for each of the large, simulated earthquakes. Source time functions for subevents of the composite earthquake model are generated based on their size. The empirical Green's functions are convolved with the source time functions to produce a suite of simulated ground motion time histories at Quebec City. Pseudo-spectral acceleration values are estimated and compared with the predicted values from ground motion models and NBCC2015 hazard values. The resultant suite of time histories for Quebec City should be representative of larger, potentially damaging, future earthquakes in the CSZ.

Keywords: synthetic strong ground motion, time histories, Quebec City, empirical Green's functions

INTRODUCTION

Strong ground motions from large earthquakes can cause significant damage to susceptible buildings. Greater Quebec City, with a population of more than 500,000 and its proximity to the CSZ seismic source zone, is at risk for potentially damaging shaking following a moment magnitude Mw 7.0, known to have occurred historically [1]. An earthquake of this magnitude will likely produce significant ground motions across a large area due to the low anelastic attenuation in the region [2]. This paper produces synthetic ground motions at Quebec City from large scenario earthquakes relevant to probabilistic design, based on the recordings of smaller earthquakes located in this area. The magnitude and distance of events were chosen based on the deaggregation of 2%/50 year hazard at Quebec City according to the 2015 seismic hazard model used in NBCC2015 [3]. The deaggregation distance of these events represents contributions from the closer part of CSZ, about 80 km from Quebec City, and the more distant part, about 160 km from Quebec City.

CHARLEVOIX SEISMIC ZONE

The Charlevoix Seismic Zone (CSZ) has the highest rate of seismicity for an intraplate setting in eastern Canada, with several large events having occurred since European settlement in the region began in the 1600s [1]. These large earthquakes resulted in the damage of several buildings in the 1800s, and geotechnical failures, such as rock falls and landslides, along the St. Lawrence River [1]. The CSZ is responsible for the largest seismic hazard values in eastern Canada [4].

The seismicity in this area has been the focus of many research projects, trying to determine the cause and types of seismicity. An early theory considered the seismicity was occurring along Logan's Line, the boundary separating Precambrian basement to the northwest and Appalachian rocks to the southeast [5]. After instrumenting the zone with a permanent network of 6 stations consisting of 3-component short-period seismometers in 1978 that provided well-constrained hypocentre locations, the seismicity was shown to occur in several bands within the Precambrian basement likely, associated with two sets of structures [1,6-8]. The first set is circular faults associated with the Charlevoix impact crater. The second set is the Paleozoic Rift faults

created during the opening of the Iapetus Ocean. These normal faults appear to be reactivated as oblique reverse-slip faults under the current regional compressional stress [9-11].

The shallow events occurring within the impact structure have a low cumulative seismic moment, lack earthquakes above M_w 4.0, and are oriented in varied directions−suggesting that the crust is highly fractured and not capable of supporting a large earthquake [8]. A large magnitude earthquake is more likely to occur along the reactivated St. Lawrence paleorift faults. There are several large mapped faults in this area striking parallel to the St. Lawrence River [12], two of which are the Charlevoix Fault and the Gouffre NW fault (CH and GNW in Figure 3 of [7]). These faults are represented by rectangular faults below 5 km, striking parallel with the river, and dipping 56° to the southeast; their shape and surface projections are shown in Figure 1.
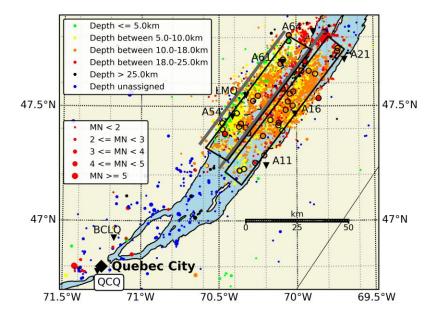

Figure 1. Map showing the location of Quebec City (black diamond), the seismic stations in CSZ and near Quebec City (inverted black triangles), the seismicity of the CSZ and surrounding region from 1990-2019, $M_N \geq 1.0$ (colored dots), and the events which passed the EGF criteria (open black circles). The surface projections of the two faults used in this study are shown as black rectangles and extrapolated to the surface, shown as thick grey lines.

EMPIRICAL GREEN'S FUNCTION DATASET

Digital seismograms from 5099 earthquakes were analyzed for use as Green's functions; however, after applying strict and rigorous criteria to ensure reliable results, 28 earthquakes remained, providing one seismogram at QCQ each. The initial selection criteria were as follows: 1) earthquakes were required to have phases picked at five or more of the surrounding stations, 2) the waveforms of the surrounding stations and those at QCQ were inspected to ensure no double events or other signals present that could interfere with the earthquake motions, and 3) the location of the hypocentre is accurate to within 5 km. Next, the pre-event signal-to-noise ratio at QCQ had to be at least 4. The signal to noise ratio is taken by calculating the RMS amplitude of a ten-second window after the S-wave arrival, and dividing it by the RMS amplitude of a ten-second window before the origin time of the earthquake. Finally, the earthquake recording was pre-processed and the instrument response removed. The resulting earthquakes used for Green's functions are listed in Table 1. They span a range of Nuttli magnitudes [13] (M_N) between M_N 2.8 to 5.4 and hypocentre distances of 85 to 160 km.

METHOD

A hundred earthquake time series are simulated to predict the possible ground motions Quebec City (site QCQ) might experience during a large (M ≥ 7.0) earthquake. The simulations are based on the 28 digital recordings made at seismograph station QCQ. This station began digital operations as a vertical component short-period seismometer in 1997 and ended in December of 2017. It is sited on rock in the basement of Pavillon Adrien-Pouliot on the campus of Université Laval, Sainte-Foy, roughly 5 km southwest of the city centre. Because the QCQ seismograph records only the vertical component of motion, the amplitudes for the synthetic ground motions are corrected to horizontal ground motions used in design. The factor of 1.15 from [14] was used to estimate horizontal components of motions. The bedrock is Paleozoic shale that has a shear wave velocity of ~1100 m/s based on similar geology elsewhere in the St Lawrence lowlands. This corresponds to Site Class B as used in

NBCC2015. Therefore, the ground motion results in this paper are considered appropriate for nearby bedrock sites in Quebec City, or as the bedrock input to the modelling of soil response where the site consists of soil over bedrock.

Table 1. List of 28 earthquakes used as Green's functions.

Date	Time	Magnitude (M_N)	Latitude	Longitude	Depth (km)
2001/05/22	00:33:29	3.5	47.654	-69.920	11.43
2003/06/13	11:34:40	4.1	47.703	-70.087	11.12
2003/08/17	06:00:03	2.9	47.555	-70.044	8.50
2003/10/11	00:10:02	3.1	47.535	-69.858	23.2
2004/04/10	05:23:18	3.2	47.826	-69.814	27.5
2004/05/29	21:21:16	3.3	47.441	-70.169	6.50
2005/03/06	06:17:49	5.4	47.753	-69.732	13.29
2006/04/07	08:31:41	4.1	47.379	-70.463	24.52
2007/09/27	11:31:08	3.3	47.411	-70.371	14.47
2008/01/03	09:37:55	3.4	47.382	-70.312	13.50
2008/11/15	10:52:54	4.2	47.739	-69.735	13.29
2009/04/12	06:48:26	3.2	47.521	-70.056	12.60
2010/03/10	06:41:18	3.1	47.685	-70.103	10.36
2010/10/07	23:10:53	3.0	47.408	-70.330	13.96
2010/10/28	23:06:09	3.0	47.427	-70.478	8.41
2011/09/27	16:47:20	2.8	47.226	-70.341	9.52
2011/11/29	17:02:25	3.4	47.547	-70.250	14.04
2012/03/25	11:30:49	2.9	47.253	-70.268	24.82
2012/04/13	10:56:51	3.0	47.696	-69.945	22.48
2012/11/01	23:28:42	2.9	47.524	-70.281	11.64
2012/12/07	17:32:30	2.9	47.565	-70.021	23.08
2012/12/12	17:46:06	4.4	47.785	-70.049	5.35
2013/07/11	20:58:10	2.8	47.811	-70.048	14.41
2013/12/11	07:47:21	3.4	47.220	-70.368	11.50
2015/01/21	05:31:59	3.7	47.371	-70.217	14.53
2015/07/12	04:17:38	2.8	47.484	-70.071	10.92
2015/09/13	00:45:18	3.1	47.425	-70.359	11.29
2016/07/29	19:55:21	3.0	47.428	-70.116	19.43

Theory

Each earthquake time series is simulated by combining a composite slip distribution based on a self-similar model [15,16] combined with Green's functions determined from regionally recorded earthquakes [17]. The velocity time series calculated from each subevent is then summed with appropriate time delays to generate a representative velocity time series of the larger earthquake and total slip. This combination of a composite slip distribution and Green's functions from recordings provides a kinematic description of slip along the fault plane with the known response of the Quebec City site from earthquakes recorded in the CSZ.

Similar methods of generating broadband time histories have been used [18-21] using the kinematic fractal source model and either a hybrid Green's function, or a synthetic Green's function. The description of our source model is identical to these studies. In our case, due to the high seismicity of the CSZ, the response at QCQ from a wide distribution of earthquakes is well represented. This creates tens of possible Green's functions that may be used without the need to generate a synthetic Green's function.

Composite Slip Model

The composite slip model uses self-similar circular slips of varying radii distributed over the fault plane [15]. The individual slips may overlap with one another [16], but are constrained to within a 30 km x 10 km plane, the approximate dimensions from a Mw 7.0 from [22]. Thus, only about 20% of the fault plane ruptures in each scenario. The number of subevents is determined based on the model described by [15] where the number of circular subevents, *N*, with radius *R* is defined by:

$$\frac{\partial N}{\partial (\ln R)} = pR^{-D} \qquad (1)$$

where D is the fractal dimension, set to 2 in this study, and p is the constant of proportionality. The maximum and minimum subevent radii are $R_{max} = 5$ km and $R_{min} = 0.1$ km respectively. If the stress drop for subevents is independent of the size of any particular subevent, then the total seismic moment of the combined event is:

$$M_0^{total} = \frac{16}{7} \Delta\sigma \sum_{i=1}^{N} R_i \tag{2}$$

using the relationship between seismic moment and the radius of an event from [23]. This leads to the value of p, as calculated by [16], to be:

$$p = \frac{7 \, M_0}{16 \, \Delta\sigma} \frac{3-D}{R_{max}^{3-D} - R_{min}^{3-D}} \tag{3}$$

Three examples of the slip distribution resulting from this model are shown in Figure 2, where the hypocentre is randomly placed within the largest subevent. Due to the orientations of the fault with respect to Quebec City, the hypocentre distance, as used in the NBCC2015 ground motion models (GMMs) [24], will be further than the closest rupture distance (taken as the upper left corner of the fault) which is the distance metric used in the GMMs proposed for the 6th Generation seismic hazard maps [25]. Considering the rectangular geometry of the rupture plane used here, the closet rupture distance will mostly be underestimated, as the upper left corner of the rupture plane will not usually have significant displacement.

The initial seismic moment in the simulated earthquakes is set to be equivalent to a moment magnitude of Mw 7.0. The stress drop varies randomly between 10-60 MPa for the large earthquakes. The stress drop is held constant between subevents during an earthquake simulation. We did not apply any constraint to keep the seismic moment at Mw 7.0, so the final earthquake can have a seismic moment larger than the expected moment due to the geometry, subevent distribution, and stress drop of the composite model. The distribution of magnitude, hypocentre distance and rupture distance is shown in Figure 3.
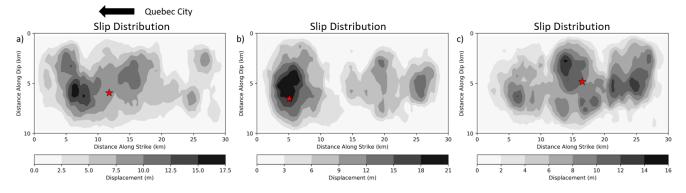

Figure 2: Displacement on the fault for three of the simulated earthquakes. Red stars indicate hypocentres. Quebec City is towards the left. The hypocentre distances for these earthquakes are 108 km, 123 km, and 166 km; the closest rupture distances are 88 km, 99 km, and 115 km for the left, middle and right earthquakes, respectively.

Empirical Green's Functions

The empirical Green's functions (EGF) used are empirical and are taken from recordings made at station QCQ, between 1999 and the present (Table 1). To be used as an EGF, the hypocentre of the earthquake must be located to within 7 kilometres of the rupture on the fault plane shown in Figure 1. Due to the high seismicity within the CSZ, it is a well-instrumented seismic zone, providing a high confidence level on the determined hypocentres.

Each recorded earthquake time series is filtered with a cosine tapered boxcar window around the S-wave arrival, and 60 seconds afterwards. Each earthquake spectrum is compared to an equivalent time windowed noise spectrum from before the event. The recorded earthquake spectra is empirically fitted with a Brune spectrum [26]. The Brune spectrum values are used for frequencies below the threshold frequency for each earthquake, based on where the spectral noise value is equal to the observed spectral value. The resulting earthquake time series is then divided by an impulse response with amplitude equal to the seismic moment of the earthquake, as determined from the M_N-M_w relation using [27].

The method results in an EGF that represents the crustal propagation, instrument response, and linear site effect of a unit impulse from the CSZ at QCQ. Several doublets of earthquakes, where similar earthquakes occur at the same location, are identified and tested to ensure that these are representative EGFs. An example is shown in Figure 4 where the EGF is nearly identical between two earthquakes, separated by 15 km in distance and nine years in time. These earthquakes have similar waveforms at surrounding stations, indicating the earthquakes have similar focal mechanisms.
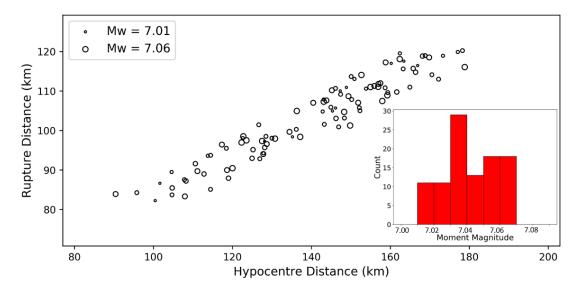
Figure 3: Closest rupture distance compared to the hypocentre distance for the simulated earthquakes. The size of the marker is representative of the moment magnitude of the simulated earthquake. The inset is the distribution of simulated earthquake magnitudes, ranging from Mw 7.0 to Mw 7.1 in 0.01 unit bins.
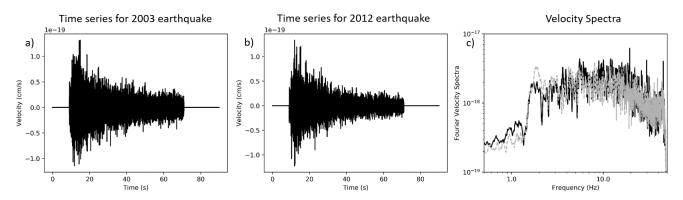

Figure 4: The velocity time series and Fourier velocity spectra for two Green's Functions from two different recordings at QCQ from earthquakes in the CSZ estimated to be 15 km apart in distance and 9 years apart in time. a) M_N 2.9 on 2003-08-17 at 06:00:38, b) M_N 2.9 on 2012-12-07 at 17:32:30, c) velocity spectra for the 2003 earthquake (black line) and for the 2012 earthquake (dashed grey line).

Velocity Time Series

The time series for a subevent is computed by convolving a source time function related to the size of the subevent [26] with the nearest EGF. The amplitude of the EGF is modified based on the distance between the station and centre of the subevent, compared to the station distance and the EGF hypocentre [19]. The geometrical spreading is assumed to be related to the inverse of the distance [28], and the frequency-dependent anelastic attenuation, $Q(f) = 758f^{0.33}$, is determined from recent studies in the region [2]. These factors are added or removed to the EGF in the frequency domain.

The resulting time series for the simulated Mw 7.0+ is calculated by summing the individual subevent time series, shifted by the time delay between the hypocentre and subevent distance. This distance is divided by the rupture velocity, 2.7 km/s, which is set to 0.8 of the crustal shear wave velocity. Sample time series are shown in Figure 5, corresponding to the slip distributions shown in Figure 2. The middle rupture represents chiefly a unilateral rupture away from Quebec City while the other two are more bilateral ruptures (as evidenced in Figure 2).
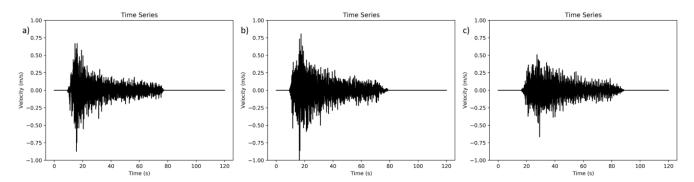
Figure 5: Three sample velocity time series of the simulated Mw 7.0 earthquakes. These time series correspond to the relative slip displacements shown in Figure 2. The PGV for the earthquakes are: left 0.873 m/s, middle 1.072 m/s, and right 0.667 m/s.

RESULTS:

The 5% damped horizontal pseudo-spectral acceleration (PSA) from the simulated earthquakes along with the high, low and median values expected for a Mw 7.0 at 80 km from the 2015 NBCC GMMs [24], and the weighted mean values for a stable crust GMM the tentative 6th Generation seismic hazard maps [25] are shown in Figure 6. The figure displays the uniform hazard spectra (UHS) for 2% in 50 years and 10% in 50 years at Quebec City. For periods above 0.2 seconds, the two GMMs are similar to one another, indicating that the comparison with their distance metrics is appropriate based on the difference between the closest rupture distance and hypocentre distance plot in Figure 3. At periods below 0.2 seconds, the simulated earthquakes display smaller PSA values than those predicted by the GMMs. The simulated earthquakes show a slight peak in PSA values at roughly 0.5 seconds, larger than that predicted by the GMMs. At periods above 1.0 seconds, the simulated earthquake PSA values are scattered about the GMM values, moving to higher-than-predicted values at 5.0 seconds and above. Overall, the scatter of PSA values straddles the high and low values of the GMMs, indicating that this suite of velocity time-series samples a realistic range of strong ground motions at Quebec City that would be associated with a large earthquake rupture in the CSZ.

CONCLUSIONS:

A collection of 100 simulated velocity time histories from a suite of earthquakes in the CSZ was generated for engineering purposes. These time series are a good match to the PSA values above 0.2 seconds that are used in the GMMs provided for the 5th and 6th generation seismic hazard maps [4,29]. It is likely that similar ground motions could be experienced at Quebec City during a future damaging earthquake from the CSZ, or quite possible were experienced during one of the large historical earthquakes, such as the 1663 earthquake.

The PSA values represent a significant portion of the values from the UHS curve for periods above 0.2 seconds. This is expected based on the deaggregation of hazard at Quebec City [3], which indicates that the hazard at these periods is influenced by larger magnitude earthquakes occurring at distances corresponding to the CSZ. The hazard at the shorter periods is dominated by smaller magnitude events at closer distances. Therefore, a larger earthquake in the CSZ would not produce the values estimated in the hazard model over the entire period range. At rupture distances of more than 80 km the shorter periods are attenuated by the crustal propagation.

The CSZ has a high level of seismicity for an intraplate setting, and several large earthquakes occurred within it during recorded history. This study uses the high seismicity and event recordings to estimate the ground motions of a larger magnitude earthquake. Using several recordings allows multiple empirical Green's functions to be used for each simulation of a larger earthquake, increasing the likelihood of capturing the complex rupture process of a large earthquake and the propagation effects between the CSZ and Quebec City.
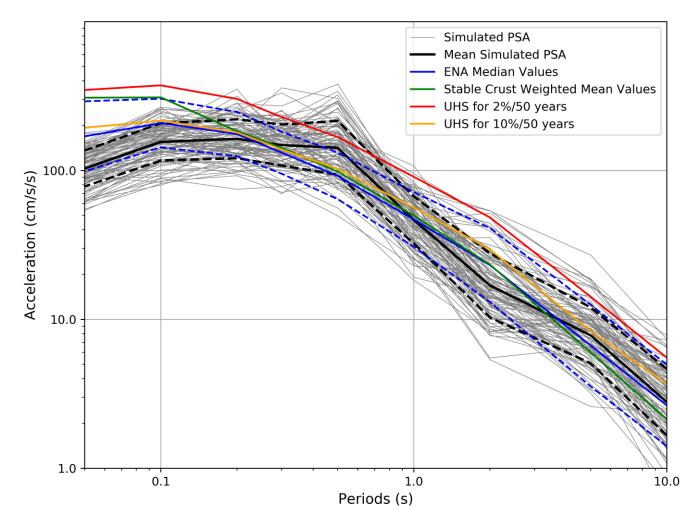
Figure 6: 5% damped horizontal PSA from the simulated Mw 7.0 earthquake time series (grey lines) at various distances along with the mean value of these simulations (black line) and the ± one standard deviation (black dashed lines). The median value (solid) and high and low values (dashed) for an Mw 7.0 at 80 km for a site class B from [24] is plotted in blue. The green line is the weighted mean GMM for the stable continental crust [25], proposed for the 6th Generation seismic hazard maps, for an Mw 7.0 at 80 km on Site Class B. The mean values of the uniform hazard spectrum (UHS) at 2% in 50 years for Quebec City [4] is plotted as a red line and the UHS for 10% in 50 years is plotted as an orange line.

ACKNOWLEDGMENTS

REFERENCES

[1] Lamontagne, M., and G. Ranalli (2014). Earthquakes and geological structures of the St. Lawrence rift system, in Intraplate Earthquakes, P.Talwani (Editor), Chap. 4, Cambridge University Press, New York, 398 pp.

[2] Perry, C., and A. Bent (2018), Regional variations in crustal seismic attenuation across Canada from Lg waveform analysis, Abstract T43F-0465 presented at 2018 Fall Meeting, AGU, Washington, D.C.,10-14 Dec.

[3] Halchuk S., J. Adams, M. Kolaj, T. Allen. (2019). Deaggregation of NBCC 2015 and 2020 Seismic Hazard for Selected Canadian Cities. 12th Canadian Conference of Earthquake Engineering, Quebec City, June 17-20, 2019. 192-DMsa-149

[4] Adams, J., Halchuk, S., Allen, T., Rogers, G. (2015). Canada's 5th Generation seismic hazard model, as prepared for the 2015 National Building Code of Canada, 11th Canadian Conference on Earthquake Engineering, 21–24 July 2015, Victoria, Canada, Paper 93775, 11pp.

[5] Leblanc, G. and G.G.R. Buchbinder (1977). Second microearthquake survey of the St. Lawrence Valley near La Malbaie, Quebec, Canada, Can. J. Earth Sci., 14, 2,778-2,789.

[6] Anglin, EM. (1984). Seismicity and faulting in the Charlevoix zone of the St. Lawrence valley, Bull. Seism. Soc. Am., 71, 1,553-1,560.

[7] Lamontagne, M., M. Beauchemin, and T. Toutin (2004). Earthquakes of the Charlevoix seismic zone, Quebec, CSEG Recorder 29, no. 8, 41–44.

[8] Yu, H., Y. Liu, R.M. Harrington, and M. Lamontagne (2016). Seismicity along St. Lawrence Paleorift Faults Overprinted by a Meteorite Impact Structure in Charlevoix, Québec, Eastern Canada, Bull. Seismol. Soc. Am., 106, no. 6, 2663–2673, doi: 10.1785/0120160036

[9] Zoback, M. L. (1992). Stress field constraints on intraplate seismicity in eastern North America, J. Geophys. Res. 97, no. B8, 11,761–11,782, doi: 10.1029/92JB00221.

[10] Adams, J. (1995). The Canadian crustal stress database—A compilation to 1994, Geol. Surv. Canada Open-File Rept. 3122, 437 pp.

[11] Mazzotti, S., and J. Townend (2010). State of stress in central and eastern North American seismic zones, Lithosphere 2, no. 2, 76–83.

[12] Lamontagne, M., P. Keating, and T. Toutin (2000). Complex faulting confounds earthquake research in the Charlevoix seismic zone, Québec, Eos Trans. AGU 81, no. 26, 289–293.

[13] Nuttli, O. W. (1973). Seismic wave attenuation and magnitude relations for eastern North America, J. Geophys. Res. 78, 876–885.

[14] Siddiqqi, J., and G. Atkinson (2002). Ground-motion amplification at rock sites across Canada as determined from the horizontal-to-vertical component ratio, Bull. Seismol. Soc. Am. 92, 877–884.

[15] Frankel, A. (1991). High-frequency spectral falloff of earthquakes, fractal dimension of complex rupture, b value, and the scaling of strength on faults, J. Geophys. Res. 96, 6291–6302.

[16] Zeng, Y., J. G. Anderson, and G. Yu (1994). A composite source model for computing realistic synthetics strong ground motions, Geophys. Res. Lett. 21, 725–728.

[17] Hartzell, S. H. (1978). Earthquakes aftershocks as Green's functions, Geophys. Res. Lett. 5, 1–4.

[18] Hutchings, L. (1994). Kinematics earthquakes models and synthesized ground motion using empirical Green's functions, Bull. Seismol. Soc. Am. 84, 1028–1050.

[19] Causse, M., E. Chaljub, F. Cotton, C. Cornou, and P.-Y. Bard (2009). New approach for coupling k−2 and empirical Green's functions: application to the blind prediction of broad-band ground motion in the Grenoble basin. Geophys. J. Int., 179, 1627–1644 doi: 10.1111/j.1365-246X.2009.04354.x

[20] Ruiz, J. A., D. Baumont, P. Bernard, and C. Berge-Thierry (2011). Modeling directivity of strong ground motion with a fractal, k-2, kinematic source model, Geophys. J. Int. 186, no. 1, 226–244, doi. 10.1111/j.1365-246X.2011.05000.x.

[21] Ruiz, J. A., D. Baumont, P. Bernard, and C. Berge-Thierry (2013). Combining a Kinematic Fractal Source Model with Hybrid Green's Functions to Model Broadband Strong Ground Motion. Bull. Seismol. Soc. Am., 103, No. 6, 3115–3130, doi: 10.1785/0120110135

[22] Somerville, P. (2014) Scaling Relations between Seismic Moment and Rupture Area of Earthquakes in Stable Continental Regions. PEER Report 2014/14

[23] Kanamori, H., and D. Anderson (1975). Theoretical basis of some empirical relations in seismology, Bull. Seismol. Soc. Am. 65, 1073–1095.

[24] Atkinson, G.M., and J. Adams (2013). Ground motion prediction equations for application to the 2015 Canadian national seismic hazard maps. Can. J. Civ. Eng., 40, 988-998. Dx.doi.org/10/1139/cjce-2012-0544

[25] Kolaj, M., Allen, T., Mayfield, R., Adams, J., and Halchuk, S. (2019). Ground-motion models for the 6th Generation Seismic Hazard Model of Canada. 12th Can. Conf. Earthquake Engineering, Quebec City, 192-hHtH-159

[26] Brune, J. N. (1970). Tectonic stress and the spectra of seismic shear waves from earthquakes, J. Geophys. Res. 75, 4997–5002.

[27] Bent, A., and H. Greene (2014). Toward an Improved understanding of the MN-Mw Time Dependence in Eastern Canada. Bull. Seismol. Soc. Am., 104, no 4, 2125-2132. doi: 10.1785/0120140031

[28] Frankel, A. (2015). Decay of S-Wave Amplitudes with Distance for Earthquakes in the Charlevoix, Quebec, Area: Effects of Radiation Pattern and Directivity. Bull. Seismol. Soc. Am., 105, 850–857. doi: 10.1785/0120140249

[29] Adams, J, Allen, T, Halchuk, S, and Kolaj M (2019). Canada's 6th Generation Seismic Hazard Model, as Prepared for the 2020 National Building Code of Canada, 12th Canadian Conference on Earthquake Engineering, Quebec, Canada, 192-Mkvp-139

[30] Beyreuther M, Barsch R, Krischer L, Megies T, Behr Y and Wassermann J (2010). ObsPy: a python toolbox for seismology Seismol. Res. Lett., 81, 530-533

[31] Hunter, J, (2007). Matplotlib is a 2D graphics package used for Python for application development, interactive scripting,and publication-quality image generation across user interfaces and operating systems. Computing in Science & Engineering, 9, 90-95. doi: 10.1109/MCSE.2007.55